Heaviside's dolphins (*Cephalorhynchus heavisidii*) relax acoustic crypsis to increase communication range

Morgan J. Martin[1], Tess Gridley[2], Simon H. Elwen[1] and Frants H. Jensen[3,4]

[1]*Mammal Research Institute, Department of Zoology and Entomology, University of Pretoria. C/o Sea Search Research and Conservation NPC, 4 Bath Rd, Cape Town 7945, South Africa*

[2] *Centre for Statistics in Ecology, Environment and Conservation, Department of Statistical Sciences, University of Cape Town. C/o Sea Search Research and Conservation NPC, 4 Bath Rd, Cape Town 7945, South Africa.*

[3]*Aarhus Institute of Advanced Studies, Aarhus University, Aarhus 8000, Denmark*

[4]*Biology Department, Woods Hole Oceanographic Institution, 266 Woods Hole Rd, Woods Hole, MA 02543, USA*

Contact: mjmartin@sandiego.edu

Field site and data collection

The study area, Shearwater Bay, located near Lüderitz in southern Namibia (-26° 37' S, 15° 05' E), is a small bay (6.5 km^2) which consists of shallow water with a maximum depth of 12 m. Data analysed in this study were collected from wild Heaviside's dolphins located in Shearwater Bay during April and May 2016.

Underwater acoustic recordings of Heaviside's dolphin vocalisations were made under calm weather conditions (Beaufort sea state ≤ 2) using two high frequency recording hydrophones (SoundTrap 300 HF; www.oceaninstruments.co.nz). The hydrophones were mounted 1 m apart and suspended 1.5 m below a 4.2 m fiberglass ocean kayak. Sound was digitised at a sampling rate of 576 kHz with a 16-bit resolution, and settings were configured to include high gain (+12 dB) and a high pass filter (400 Hz), effective sensitivity: -171 dB *re* 1 V/µPa, flat frequency response: 400 Hz – 150 kHz ± 3 dB. A built in anti-aliasing filter exists at 150 kHz. Recordings were stored as compressed 30-min SUD files on the SoundTraps.

The kayak and hydrophone array were deployed when Heaviside's dolphins were observed from shore and weather conditions permitted. When an individual or group of dolphins was sighted, the observer on board the kayak would attempt to approach with minimal disturbance. A group was defined as two or more dolphins in close proximity (< 50 m radius), generally carrying out the same activity. Behaviour and focal group information were collected concurrently with sound recordings using a Dictaphone. A visual survey group-follow with incident sampling protocol [1, 2] was used to record surface behaviour along with group size, group composition (presence or absence of calves), group spacing, and estimated distance from the hydrophone array. Definitions

of behavioural states and events were adapted from [3, 4]. A secondary visual survey method was implemented from shore (20 m elevation) using two observers with walkie talkies and a Sony Handycam camcorder to assist the kayak-based observer to locate and maintain focal groups, monitor other Heaviside's dolphin groups present in the bay, provide information on behaviour and to assess inter-observer reliability [5].

Statistical analyses

All high-quality measured signals visually classified into the four proposed categories were evaluated to examine the ability to quantitatively distinguish pulsed signal types. Signal parameters were compared across signal categories using non-parametric Kruskal-Wallis tests and subsequent Dunn's post-hoc tests for pairwise comparisons in R version 3.4.2 [6, 7] (Suppl. Table 1). Further in R, all high-quality signals were evaluated with a principal component analysis (PCA) as it is robust to correlated variables. The PCA was used to identify the most influential parameters for signal classification. Nine parameter variables were included in the PCA: 5^{th}, median (50^{th}) and 95^{th} percentile interclick intervals (ICI), peak frequency, centroid frequency, -10 dB bandwidth, RMS bandwidth, Q-ratio, and -10 dB click duration (Suppl. Fig. 1). All values were log-transformed prior to the analysis. The Kaiser criterion was used to identify the number of principal components to retain and was determined by eigenvalues > 1 (Suppl. Table 2). We then used a Random Forest classifier [8] to measure prediction accuracy as a function of buzz and burst-pulse signal categories using either interclick intervals (5^{th}, 50^{th} and 95^{th} percentiles for each signal), spectral and temporal click parameters (peak frequency, centroid frequency, -10 dB bandwidth, RMS bandwidth, Q-ratio, and -10 dB click duration), or all parameters combined as features to test the potential benefit of spectral differences in decreasing signal ambiguity in the repertoire. The Random Forest classifier was built in MATLAB 2017b using a 'bagged trees' ensemble classifier with 30 learners. Prediction accuracy was measured using 5-fold cross-validation to prevent overfitting. To measure consistency in prediction accuracy, the classifier was trained 100 times and prediction accuracy was measured for each iteration.

Supplementary Table 1. Dunn's post-hoc tests of measured parameters across signal categories. All parameters were log-transformed before statistical analysis. Note that initially click trains were differentiated visually from buzzes and burst-pulses using click rates with interclick intervals exceeding 10 ms. A subset of click trains were composed of lower-frequency, broader bandwidth signals than previously described [9], and we therefore divided click trains into NBHF click trains and broadband click trains by inspecting spectrograms. Initially, buzz and burst-pulse signals were visually differentiated by the presence or absence of a preceding click train as burst-pulses occur as isolated signals.

	ICI_{5th}	**ICI_{MED}**	**ICI_{95th}**	**F_P**	**F_C**	**BW_{10dB}**	**BW_{RMS}**	**Q_{RMS}**	**Dur_{10dB}**
Signal Comparison	*p*	*p*	*p*	*p*	*p*	*p*	*p*	*p*	*p*
NBHF Train : BB Train	0.9695	0.8520	0.6452	**< 0.0001**	**< 0.0001**	**< 0.0001**	**< 0.0001**	**< 0.0001**	**< 0.0001**
NBHF Train : Buzz	**< 0.0001**	**< 0.0001**	**< 0.0001**	0.1466	0.7288	0.3543	**0.0062**	**0.0189**	0.4201
NBHF Train : Burst-pulse	**< 0.0001**	**< 0.0001**	**< 0.0001**	**< 0.0001**	**< 0.0001**	**< 0.0001**	**< 0.0001**	**< 0.0001**	**< 0.0001**
Buzz : Burst-pulse	**< 0.0001**	**< 0.0001**	**< 0.0001**	**< 0.0001**	**< 0.0001**	**< 0.0001**	**< 0.0001**	**< 0.0001**	**< 0.0001**
Buzz : BB Train	**< 0.0001**	**< 0.0001**	**< 0.0001**	**0.0029**	**< 0.0001**	**< 0.0001**	**0.0002**	**< 0.0001**	**< 0.0001**
Burst-pulse : BB Train	**< 0.0001**	**< 0.0001**	**< 0.0001**	0.7380	0.4669	0.5611	0.9823	0.6735	**0.0459**

$\alpha = 0.05$, *p*-values below this threshold are shown in boldface

Abbreviations: NBHF Train = narrowband high-frequency click train; BB Train = broadband click train; ICI_{5th}, ICI_{MED} and ICI_{95th} = 5^{th}, median (50^{th}) and 95^{th} percentile interclick intervals (ms); F_P = peak frequency (kHz); F_C = centroid frequency (kHz); BW_{10dB} = -10 dB bandwidth (kHz); BW_{RMS} = root mean square bandwidth (kHz); $Q_{RMS} = F_C/BW_{RMS}$; Dur_{10dB} = -10 dB click duration (µs)

Supplementary Table 2. PCA output of the nine measured parameter variables from 159 signals. All parameter values were log-transformed prior to the PCA. Parameter abbreviations: $ICI_{5th,}$ ICI_{MED} and ICI_{95th} = 5^{th}, median (50^{th}) and 95^{th} percentile interclick intervals (ms); F_P = peak frequency (kHz); F_C = centroid frequency (kHz); BW_{10dB} = -10 dB bandwidth (kHz); BW_{RMS} = root mean square bandwidth (kHz); $Q_{RMS} = F_C/BW_{RMS}$; Dur_{10dB} = -10 dB click duration (µs)

	PC1	**PC2**	**PC3**	**PC4**	**PC5**	**PC6**	**PC7**	**PC8**	**PC9**
Importance of Components									
Standard Deviation	2.099	1.545	1.088	0.794	0.461	0.383	0.172	0.058	0.010
Prop. of Variance	0.490	0.265	0.132	0.070	0.024	0.016	0.003	0.000	0.000
Cumulative Prop.	0.490	0.755	0.886	0.956	0.980	0.996	1.000	1.000	1.000
Loadings with Rotation = (9 x 9)									
ICI_{5th}	-0.326	-0.460	0.104	-0.037	0.063	0.050	-0.602	-0.548	-0.005
ICI_{MED}	-0.329	-0.459	0.116	-0.056	0.045	0.031	-0.166	0.797	0.002
ICI_{95th}	-0.328	-0.451	0.126	-0.058	-0.009	-0.010	0.777	-0.255	0.003
F_P	-0.254	0.332	0.514	0.231	0.704	-0.107	0.026	-0.002	-0.001
F_C	-0.226	0.306	0.619	-0.160	-0.585	0.252	-0.035	-0.002	0.201
BW_{10dB}	0.369	-0.218	0.398	0.000	-0.173	-0.791	-0.048	-0.001	0.001
BW_{RMS}	0.405	-0.139	0.328	-0.361	0.144	0.359	0.018	-0.002	-0.656
Q_{RMS}	-0.426	0.210	-0.124	0.280	-0.292	-0.255	-0.019	0.007	-0.728
$Duration_{10dB}$	-0.284	0.244	-0.179	-0.840	0.141	-0.320	-0.017	-0.008	0.000

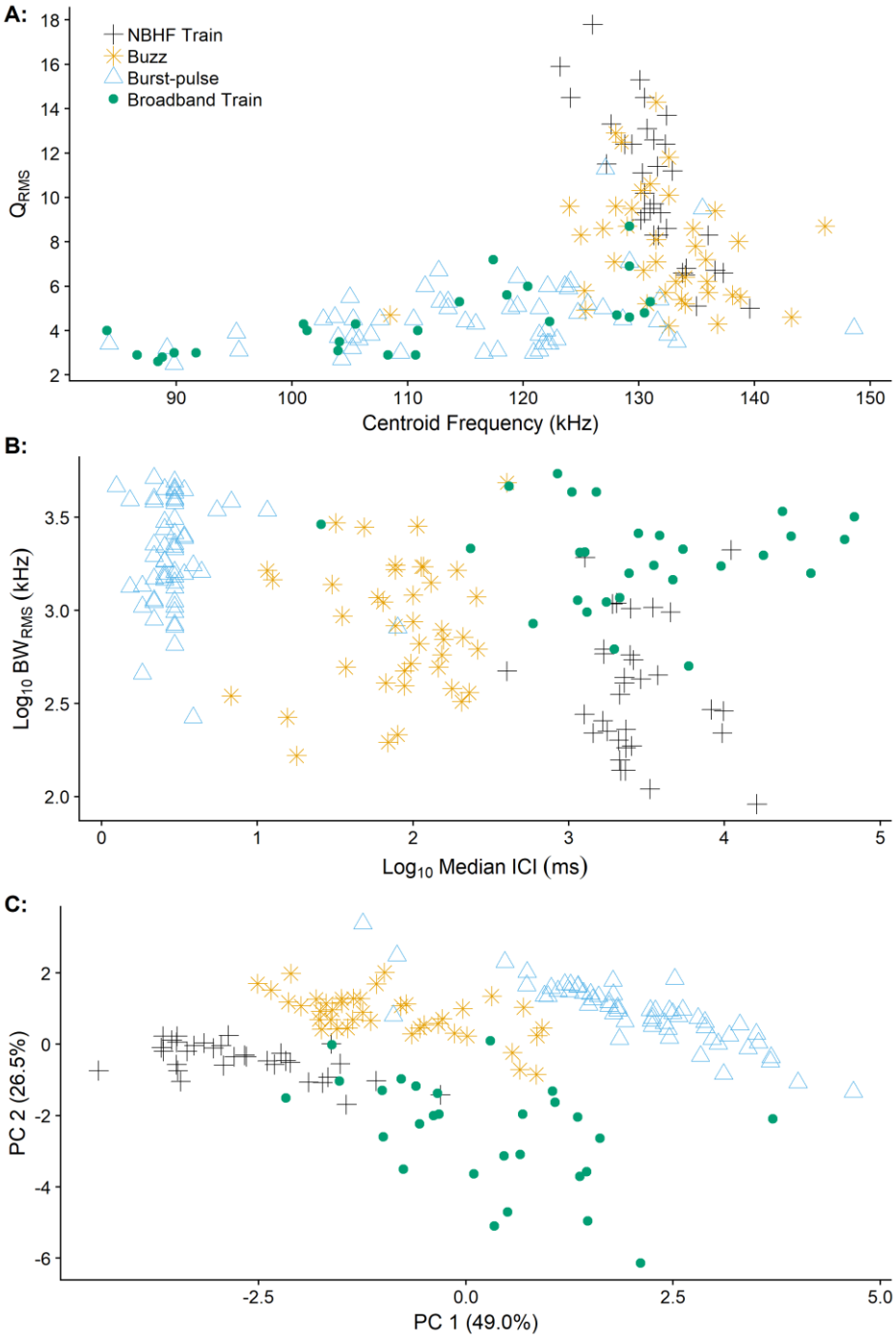

Suppl. Fig. 1: Signal parameters and discrimination of signal types. A: Q-ratio (centroid frequency / RMS bandwidth) as a function of centroid frequency. B: Log-transformed RMS bandwidth as a function of log-transformed median ICI. C: Principal component analysis of signal types including nine parameter variables. Each data point represents one measured pulsed signal. PC 1 primarily represents RMS bandwidth and Q-ratio parameters. PC 2 represents click rate parameters (5^{th}, 50^{th} and 95^{th} percentile interclick intervals).

Acoustical modelling of detection range and impact on active space

To investigate how click type affects conspecific detection range and active space, we built an acoustic model of detection range under a noise-limited scenario using the passive sonar equation [10] and assuming successful detection when received sound energy exceeded masking noise energy integrated across auditory bandwidth:

Eq. 1: $$RL = SL - TL > NL$$

Here, RL is the received echo level, SL is the source level measured in energy flux density, TL is the transmission loss between source and receiver, NL is the masking noise level; all in decibels.

Since toothed whales have directional sound emission and directional hearing, we modelled detection range explicitly as a function of the outgoing source angle θ_S and the incoming receiver aspect θ_R. Directional sound emission was modelled through a transmission gain (TG), the difference between off-axis apparent source level and the on-axis source level, with values always negative. Directional hearing was modelled through an auditory gain (AG), the difference between off-axis hearing sensitivity and on-axis hearing sensitivity, with values always negative.

Eq. 2: Successful detection when: $SL + TG(\theta_S) - TL + AG(\theta_R) > NL$

Source level: On-axis source level for Heaviside's dolphin NBHF clicks has been measured to 161±5 dB [min 149, max 174] re. 1 µPa RMS for a -10 dB duration of 74 µs [9]. To reflect the temporal integration of the auditory system, we corrected these source levels for a temporal integration time of 264 µs for a bottlenose dolphin [11] by adding $10log_{10}(74\mu s/264\mu s)$.

Directional sound emission: Off-axis apparent source level was modelled using a circular, symmetric piston which has frequently been used to approximate the sonar beam of toothed whales [12]. Transmission beams were calculated for 10 NBHF clicks and 9 burst-pulse clicks using a piston size of 6.4 cm diameter and a waveform filtered with a 10 kHz - 150 kHz 6-pole Butterworth bandpass filter (Fig. 3A). This resulted in a directivity index (DI_T) of 24 dB for NBHF clicks, similar to that of other NBHF species [13-15] and decreasing to 20 dB for burst-pulse clicks. For the rest of the paper, we used a model burst-pulse click with a centroid frequency of 80 kHz[1] to calculate the possible change in detection range. We assumed that animals were energy limited and that a change in directivity would therefore lead to a lower on-axis source level, so on-axis SL for burst-pulse clicks was set 4 dB lower than for NBHF clicks.

Transmission loss: We estimated transmission loss as the combination of spherical spreading loss and frequency dependent absorption, so that TL = 20 $\log_{10}$(R) + αR. Here, R was the range to the target (m), and the absorption coefficient α was calculated using the centroid frequency of each

[1] Note that click parameters reported in manuscript are for signals filtered with a wider bandwidth Butterworth filter (20 kHz – 275 kHz), and centroid frequency measurements here are therefore similar but not directly comparable.

click type [16], resulting in an absorption coefficient of 0.40 dB/m for a 128 kHz NBHF click and 0.22 dB/m for an 80 kHz burst-pulse click.

Directional hearing: No data were available for hearing directivity at the exact frequencies required. Instead, we used auditory sensitivity measurements as a function of angle reported for a harbour porpoise (*Phocoena phocoena*) at 64 kHz and 100 kHz [17], which represents a similar shift in frequency (a little over half an octave) as the difference between NBHF and burst-pulse clicks. While this study found a slightly asymmetric receiving beam, we simplified this by taking the mean acoustic sensitivity between the left and right side, and then interpolated across values using a piecewise cubic interpolation. This resulted in a receiver directivity index (DI_R) of 8.8 dB (100 kHz) and 5.1 dB (64 kHz; Suppl. Fig. 2).

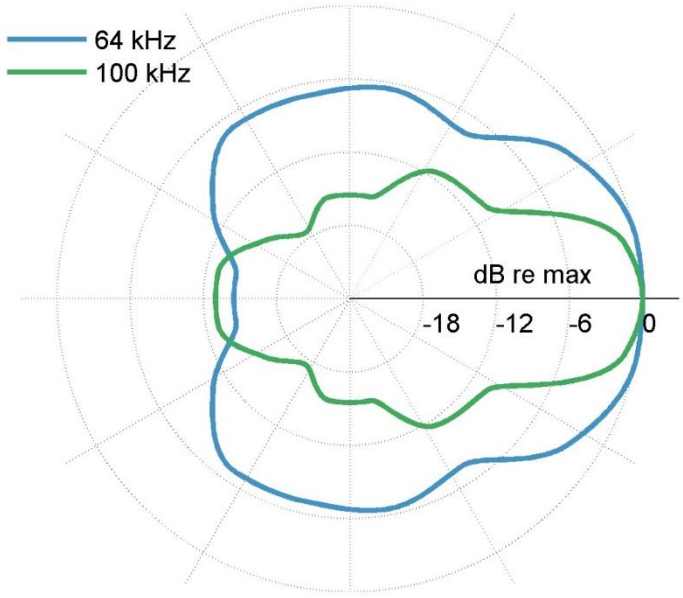

Suppl. Fig. 2: Aspect dependent hearing sensitivity (implemented here as auditory gain AG) based on measurements from a harbour porpoise [17].

Masking noise level: The masking noise energy was estimated as the spectral noise level N_0 (in dB re 1 µPa^{2}Hz^{-1}, i.e. noise intensity per Hz bandwidth) integrated over the auditory filter bandwidth of the animal and suppressed by the auditory directivity of the animal. Since we did not have reliable estimates of auditory filter bandwidth for clicks, we assumed a simple 1/3rd octave bandwidth similar to terrestrial mammals:

Eq. 3: $$NL = N_0(F_c) + 10log_{10}(0.23 * F_C) - DI_R$$

The spectral noise level was estimated as Wenz Sea State 2 deep-water noise levels (approximately 58 dB at 1 kHz, with a gradual decrease of 17 dB per decade increase in frequency), plus the addition of thermal noise (generally at frequencies above 100 kHz) (both in dB re. 1 µPa^{2}Hz^{-1}):

Eq. 4: $$N_0(F_c) = \underbrace{N_0(1\,kHz) - 17log_{10}\left(\frac{F_c}{1\,kHz}\right) - 75}_{\text{----(wind generated noise)---}} + \underbrace{20log_{10}(F_c)}_{\text{---(thermal noise)---}}$$

Equations from http://www.usna.edu/Users/physics/ejtuchol/documents/SP411/Chapter11.pdf

Detection range: We solved equation 2 numerically in MATLAB 2013b to find the maximum detection range where the received level exceeded the masking noise level. The detection range was calculated as a function of source angle (θ_S) and receiver aspect (θ_R), for both a NBHF click and an 80 kHz burst-pulse click (Suppl. Fig. 3).

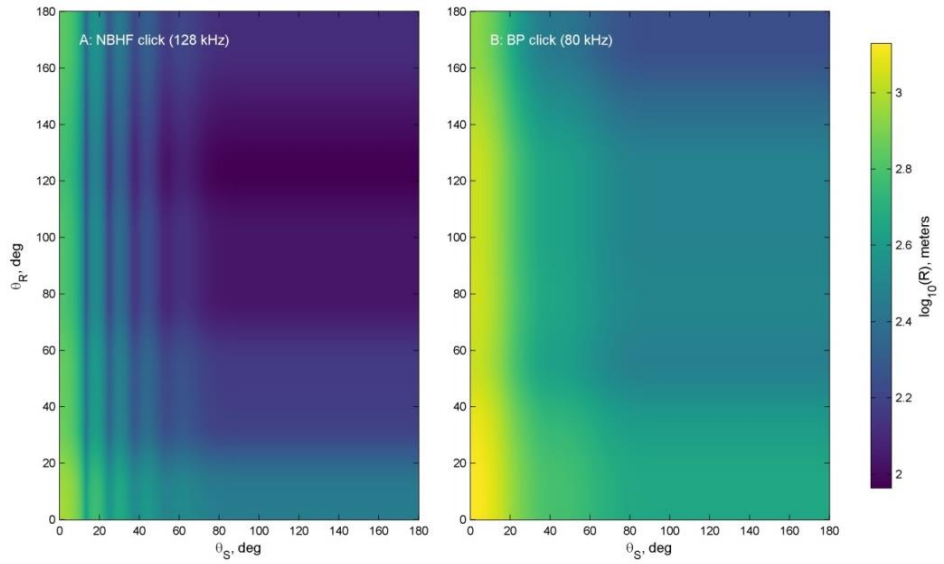

Suppl. Fig. 3: Modelled conspecific detection range for a Heaviside's dolphin NBHF click and an 80 kHz burst-pulse click, as a function of both source angle and receiver aspect.

Active space: To calculate active space, we assumed a 2D habitat with conspecifics located at the water surface. We then calculated the total detection area A (m^2) by integrating detection range R as a function of source angle from 0 to 180 degrees and assuming rotational symmetry:

Eq. 5: $$A = 2\int_0^{\pi} R(\theta_s)\sin d\theta_s$$

Since detection range depends both on source angle θ_S and receiver aspect θ_R, we assumed an equal probability of receiver aspect and used the mean detection range as a function of receiver aspect, so only source angle appears in equation 5.

Sensitivity analysis: The two most important parameters for detection range are source level and noise level. We therefore conducted a sensitivity analysis to measure the change in total detection area (A_{BP}/A_{NBHF}) across a wide range of possible source levels and noise levels. We varied wind-generated noise [N_0(1kHz)] from 50 to 75 dB re. 1 μPa^2Hz^{-1} while keeping thermal noise constant, thus increasingly favouring NBHF signals that are primarily limited by thermal noise. We used 5 different source levels reflecting the full range of NBHF source levels measured empirically from Heavisides dolphins [9]. For all simulations, the modelled active space for burst pulse signals was at least twice as large, and for quieter (Sea State 1 or Sea State 2 conditions) as high as 4 to 5 times as large as for NBHF signals.

References

1. Altmann J. Observational study of behaviour: sampling methods. *Behaviour*. 1974. **49**: 227-67.
2. Mann J. Behavioural sampling methods for cetaceans: A review and critique. *Mar. Mamm. Sci*. 1999. **15**: 102-22.
3. Herzing DL. Vocalizations and associated underwater behavior of free-ranging Atlantic spotted dolphins, *Stenella frontalis*, and bottlenose dolphins, *Tursiops truncatus*. *Aquat. Mamm*. 1996. **22**: 61-79.
4. Henderson EE, Hildebrand JA, Smith MH, Falcone EA. The behavioral context of common dolphin (*Delphinus sp*.) vocalizations. *Mar. Mamm. Sci.* 2011. **28**: 439-60. (doi:10.1111/j.1748-7692.2011.00498.x)
5. Kaufman AB, Rosenthal R. Can you believe my eyes? The importance of interobserver reliability statistics in observations of animal behaviour. *Anim. Behav.* 2009. **78**: 1487-91.
6. Fox J, Weisberg S. *An R Companion to Applied Regression, 2nd Ed.* Thousand Oaks, California: Sage Publications. 2011.
7. Ogle D. FSA: Fisheries Stock Analysis. R package version 0.8.16. 2017.
8. Breiman L. Random Forests. *Machine learning*. 2001. **45**: 5-32. (doi:10.1023/A:1010933404324)
9. Morisaka T, Karczmarski L, Akamatsu T, Sakai M, Dawson S, Thornton M. Echolocation signals of Heaviside's dolphins (*Cephalorhynchus heavisidii*). *J. Acoust. Soc. Am.* 2011. **129**: 449-57. (doi:10.1121/1.3519401)
10. Au W. *The Sonar of Dolphins*. New York: Springer-Verlag. 1993. (doi:10.1007/978-1-4612-4356-4)
11. Au WW, Moore PW, Pawloski DA. Detection of complex echoes in noise by an echolocating dolphin. *J. Acoust. Soc. Am.* 1988. **83**: 662-8.
12. Jensen FH, Wahlberg M, Beedholm K, Johnson M, de Soto NA, Madsen PT. Single-click beam patterns suggest dynamic changes to the field of view of echolocating Atlantic spotted dolphins (*Stenella frontalis*) in the wild. *J. Exp. Biol.* 2015. **218**: 1314-24. (doi:10.1242/jeb.116285)
13. Kyhn LA, Tougaard J, Jensen F, Wahlberg M, Stone G, Yoshinaga A, et al. Feeding at a high pitch: source parameters of narrow band, high-frequency clicks from echolocating off-shore hourglass dolphins and coastal Hector's dolphins. *J. Acoust. Soc. Am.* 2009. **125**: 1783-91. (doi:10.1121/1.3075600)
14. Kyhn LA, Jensen FH, Beedholm K, Tougaard J, Hansen M, Madsen PT. Echolocation in sympatric Peale's dolphins (*Lagenorhynchus australis*) and Commerson's dolphins (*Cephalorhynchus commersonii)* producing narrow-band high-frequency clicks. *J. Exp. Biol.* 2010. **213**: 1940-9. (doi:10.1242/jeb.042440)
15. Kyhn LA, Tougaard J, Beedholm K, Jensen FH, Ashe E, Williams R, et al. Clicking in a killer whale habitat: narrow-band, high-frequency biosonar clicks of harbour porpoise (*Phocoena phocoena*) and Dall's porpoise (*Phocoenoides dalli*). *PLOS ONE*. 2013. **8**: e63763. (doi:10.1371/journal.pone.0063763)
16. Kinsler LE, Frey AR, Coppens AB, Sanders JV. *Fundamentals of Acoustics, 4th Ed.* Wiley-VCH. 1999. p. 560.
17. Kastelein RA, Janssen M, Verboom WC, de Haan D. Receiving beam patterns in the horizontal plane of a harbor porpoise (*Phocoena phocoena*). *J. Acoust. Soc. Am.* 2005. **118**: 1172-9. (doi:10.1121/1.1945565)